Ionic Partition Diagrams: A Potential−pH Representation

Frédéric Reymond,[†] Guillaume Steyaert,[‡] Pierre-Alain Carrupt,[‡] Bernard Testa,[‡] and Hubert Girault*[,†]

Contribution from the Laboratoire d'Electrochimie, Ecole Polytechnique Fédérale de Lausanne, CH-1015 Lausanne, Switzerland, and Institut de Chimie Thérapeutique, Section de Pharmacie, Université de Lausanne, CH-1015 Lausanne, Switzerland

Received June 27, 1996[⊗]

Abstract: A general method to predict and interpret the transfer mechanisms of ionizable compounds at the interface between two immiscible electrolyte solutions (ITIES) is presented. The approach is based on the construction of the ionic partition diagram of the solute. It consists in defining equiconcentration boundaries as a function of the Galvani potential difference and aqueous pH by taking into account the thermodynamic equilibria governing the distribution of the various acid/base forms of the molecules involved. The method defines the domains of predominance of each species either in the aqueous or in the organic phase. The application of ionic partition diagrams to quinidine offers a global and direct visualization of all the species and demonstrates the validity and efficiency of the method in helping to understand the transfer and partition mechanisms of ionizable drugs.

1. Introduction

When two immiscible liquid phases are brought in contact, a distribution of the different species, neutral and ionic, spontaneously occurs. The partition of neutral species depends primarily on the nature of the solvents, whereas the partition of ionic species is restricted by the fact that the electroneutrality must be maintained in the two adjacent phases. Furthermore, the partition of ions results in a difference of inner potentials between the two phases, this difference being called the Galvani potential difference. The detailed knowledge of the distribution of acid/base in biphase liquid systems is important to many fields such as solvent extraction, phase transfer catalysis, or drug lipophilicity and its consequences to drug delivery. The latter aspect is at the origin of the present work.

Cyclic voltammetry and centrifugal partition chromatography are recently introduced techniques to study the transfer and partition mechanisms of ionic drugs at the interface between two immiscible electrolyte solutions (ITIES).[1−4] These two techniques allow the partition coefficients of both neutral and ionic forms of drugs to be determined and can lead to a complete description of the thermodynamic cycle governing transfer and partition.[5] Because it does not neglect the partitioning of ionic species, such a global approach offers a better understanding of the physicochemical mechanisms of passive transfer of organic ions. As a result, the approach can yield a quantitative description of the lipophilicity of ionic drugs and hence an improved understanding of the disposition of drugs in the body (*i.e.*, their pharmacokinetic behavior).[6]

Electrochemistry at the ITIES is a powerful and specific tool allowing quantification of the passive transfer and partition of ions across the interface. This partitioning is potential- and pH-dependent, and the presence of a species in one phase thus depends directly on the aqueous pH and on the potential applied across the interface. To obtain a global view of these phenomena, it would be of great utility to know which species is favored under given conditions of Galvani potential difference and pH. In this manner, it would become easy to predict qualitatively the influence of a change in potential or pH on the concentrations of the various species and thus to determine the nature of the transferring ions.

In this paper, we present a new approach that makes such predictions possible by drawing what we call here "ionic partition diagrams". The method consists of representing the domains of predominance of the various species as a function of applied potential and aqueous pH. The paper establishes the theoretical bases of ionic partition diagrams and demonstrates their utility with the ionizable drug quinidine as a case in point.

2. Theory

The construction of the partition diagram of an ionizable solute follows the well-known potential *versus* pH diagrams developed by Pourbaix[7] to study the corrosion of metals in acido-basic solutions under oxidoreductive conditions. Since much of the methodology used to study charge transfer reactions at metallic electrode/electrolyte solution interfaces[8] may be used in studies at the liquid/liquid interface,[9] the drawing of ionic partition diagrams is then similar to that of potential−pH diagrams of metals. The same treatment is applied here to the general case of an amphoteric molecule liable to liquid/liquid partitioning. The procedure followed is described in detail in the Supporting Information, and only the principles for the construction of ionic partition diagrams are given here.

Let us consider the case of a solute HA, which can be protonated twice in acidic solution to form HAH^+ and HAH_2^{2+},

[†] Ecole Polytechnique Fédérale de Lausanne.

[‡] Université de Lausanne.

[⊗] Abstract published in *Advance ACS Abstracts,* November 1, 1996.

(1) Solomon, T. *J. Electroanal. Chem.* **1991**, *313*, 29−35.

(2) Arai, K.; Ohsawa, M.; Kusu, F.; Takamura, K. *Bioelectrochem. Bioenerg.* **1993**, *31*, 65−76.

(3) Wang, E.; Wang, H.; Yu, Z. *Electroanalysis* **1994**, *6*, 1020−1023.

(4) Tsai, R.-S.; Carrupt, P.-A.; Testa, B. Measurement of Partition Coefficients Using Centrifugal Partition Chromatography. In *Modern Countercurrent Chromatography*; Conway, W. D., Petroski, R. J., Eds.; American Chemical Society: Washington, DC, 1995; Vol. 593, pp 143−154.

(5) Reymond, F.; Steyaert, G.; Carrupt, P.-A.; Testa, B.; Girault, H. H. *Helv. Chim. Acta* **1996**, *79*, 101−117.

(6) Fenstermacher, J. D. Drug Transfer across the Blood-Brain Barrier. In *Topics of Phamaceutical Sciences*; Breimer, D. D., Speiser, P., Eds.; Elsiever: Amsterdam, 1983; pp 143−154.

(7) Pourbaix, M. *Atlas d'Equilibres Electrochimiques*; Gauthier-Villars: Paris, 1963; pp 644.

(8) Bard, A. J.; Faulkner, L. R. *Electrochemical Methods: Fundamentals and Applications*; J. Wiley & Sons: New York, 1980; pp 213−248.

(9) Girault, H. H.; Schiffrin, D. J. Electrochemistry of Liquid/Liquid Interfaces. In *Electroanalytical Chemistry*; Bard, A. J., Ed.; Marcel Dekker: New York and Basel, 1989; Vol. 15, pp 1−141.

S0002-7863(96)02187-7 CCC: $12.00

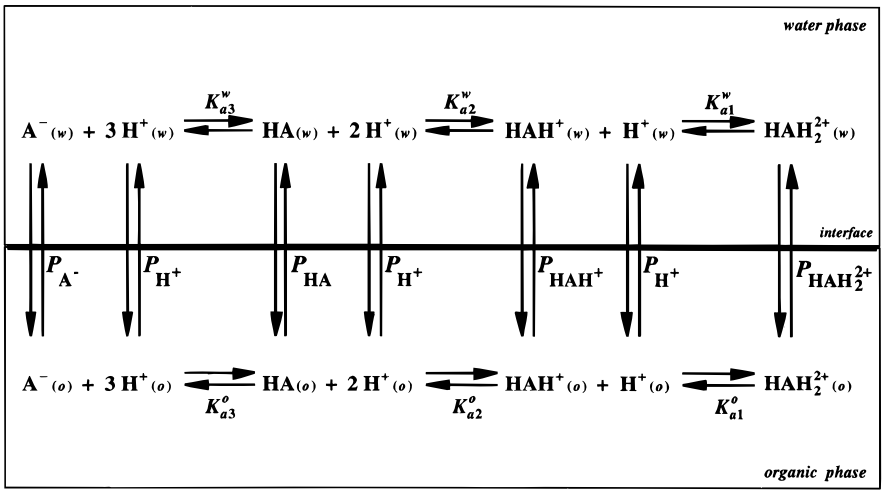

Figure 1. Thermodynamic equilibria for the transfer of A. K_a^w and K_a^o are the dissociation constants in the water and the organic phase, respectively, and P_i is the partition coefficient of i between the two phases.

and which can be deprotonated into A^- in basic solution. Since the aqueous phase is in contact with the organic phase, HA can partition between the two phases, so that the transfer process of the solute is entirely determined by the thermodynamic cycle described in Figure 1.

All of the species appearing in this thermodynamic cycle are bound together by three different types of equations, which are further used to determine equiconcentration or "boundary" lines defining the domain of predominance of each species involved:

(1) For reversible (*i.e.*, kinetically fast) ion transfer reaction, the partition of the ionized form of a species is described by the Nernst equation for the ITIES:[10]

$$\Delta_o^w\phi = \Delta_o^w\phi_i^0 + \frac{RT}{z_iF}\ln\left(\frac{a_i^o}{a_i^w}\right) = \Delta_o^w\phi_i^{0'} + \frac{RT}{z_iF}\ln\left(\frac{c_i^o}{c_i^w}\right) \quad (1)$$

where $\Delta_o^w\phi$ is the Galvani potential difference between the organic (o) and the aqueous (w) phases, c_i^o and c_i^w are the concentrations in the organic and water phases, respectively, $\Delta_o^w\phi_i^0$ is the standard ion transfer potential of the ionic species i, which is in fact the standard Gibbs energy of transfer expressed in a potential scale ($\Delta_o^w\phi_i^0 = \Delta G_{tr,i}^{0,w\to o}/z_iF$), and $\Delta_o^w\phi_i^{0'}$ is the formal ion transfer potential which can be determined experimentally.

The ratio c_i^o/c_i^w represents the partitioning of the ionic species i between the two phases, P_i. It is potential-dependent[5] and may be deduced from eq 1:

$$\log P_i = \log\left(\frac{c_i^o}{c_i^w}\right) = \frac{z_iF}{2.303RT}(\Delta_o^w\phi - \Delta_o^w\phi_i^{0'}) = \log P_i^0 + \frac{ziF}{2.303RT}\Delta_o^w\phi \quad (2)$$

where $\log P_i^0$ is the standard partition coefficient of the ionic species i.

When the concentrations of two contiguous species are equal, the term $\log(c_i^o/c_i^w)$ is zero in eqs 1 and 2. The Nernst equations simplify then into

$$\Delta_o^w\phi = \Delta_o^w\phi_i^{0'} \quad (3)$$

resulting in boundary lines parallel to the pH axis with an ordinate equal to the formal transfer potential of the respective ion.

(2) The partition of a neutral species HA is a unique quantity related to the Gibbs transfer energy of the species and is defined by

$$\log P_{HA} = \log\left(\frac{c_{HA}^o}{c_{HA}^w}\right) = -\frac{\Delta G_{tr,HA}^{0,w\to o}}{2.303RT} \quad (4)$$

This relationship is neither potential- nor pH-dependent, so that it does not determine any boundary line. Consequently, c_{HA}^w and c_{HA}^o cannot appear simultaneously on the ionic partition diagram and a choice must be made in order to choose the parameter to be used in the calculations.

By convention, c_{HA}^w is chosen as the variable, so that the domain of predominance of HA(w) appears on the ionic partition diagram. This choice is arbitrary, but it influences the shape of the diagram. However, it should be kept in mind that both HA(w) and HA(o) are present in the electrochemical system, even if only one of the two appears in the ionic partition diagram. This fact must be taken into account when ionic partition diagrams are used to interpret transfer and partition mechanisms.

(3) The various acid−base equilibria (Figure 1) delimit the boundaries between two ions differing in electrical charge. In the aqueous phase, the concentration ratio between two ions of different charge may directly be deduced from the thermodynamic definition of the dissociation constants K_a^w. As an example, the equilibria between the doubly and singly positively charged species is given by eq 5, where the ratio of the activity coefficients is neglected:

$$HAH_2^{2+}(w) \rightleftarrows HAH^+(w) + H^+(w): \quad \log\left(\frac{c_{HAH^+}^w}{c_{HAH_2^{2+}}^w}\right) = \mathrm{pH} - \mathrm{p}K^w{}_{a1} \quad (5)$$

When the concentrations of the various species are equal, all the acid−base equilibria reduce to

$$\mathrm{pH} = \mathrm{p}K_a^w \quad (6)$$

Equation 6 thus defines three additional boundary lines which are parallel to the ordinate axis and independent of $\Delta_o^w\phi$.

(10) Girault, H. H. Charge Transfer across Liquid/Liquid Interfaces. In *Modern Aspects of Electrochemistry*; Bockris, J. O'M., Conway, B., White, R., Eds.; Plenum Press: New York, 1993; Vol. 25, pp 1−62.

In the organic phase, the dissociation constants, K_a^o, can be defined by eqs 7:

$$K_{a1}^o = \frac{c_{HAH^+}^o c_{H^+}^o}{c_{HAH_2^{2+}}^o}; \quad K_{a2}^o = \frac{c_{HA}^o c_{H^+}^o}{c_{HAH^+}^o}; \quad K_{a3}^o = \frac{c_{A^-}^o c_{H^+}^o}{c_{HA}^o} \qquad (7)$$

In order to appear on the ionic partition diagram, the proton concentration in the organic phase must be replaced in eqs 7 by the pH in the aqueous phase. This is accomplished by substitution of $c_{H^+}^o$ by the Nernst equation for the proton given by eq 8:

$$\log(c_{H^+}^o) = \frac{F}{2.303RT}(\Delta_o^w\phi - \Delta_o^w\phi_{H^+}^{0'}) - \mathrm{pH} \qquad (8)$$

Furthermore, in order to be consistent with the convention adopted here, c_{HA}^o cannot appear in the expressions of the boundary lines. Using the definition of the partition of neutral species (eq 4) and the Nernst equation for the proton, the potential dependence of the various species of A in the organic phase can thus be evaluated. This yields the boundaries between HAH_2^{2+}(o) and HAH^+(o), HAH^+(o) and HA(w), and HA(w) and A^-(o), respectively, defined by eqs 9−11.

$$\Delta_o^w\phi = 2\Delta_o^w\phi_{HAH_2^{2+}}^{0'} - \Delta_o^w\phi_{HAH^+}^{0'} + \frac{2.303RT}{F}(\mathrm{pH} - \mathrm{p}K_{a1}^w) + \frac{2.303RT}{F}\log\left(\frac{c_{HAH_2^{2+}}^o}{c_{HAH^+}^o}\right) \qquad (9)$$

$$\Delta_o^w\phi = \Delta_o^w\phi_{HAH^+}^{0'} + \frac{2.303RT}{F}(\mathrm{pH} - \mathrm{p}K_{a2}^w) + \frac{2.303RT}{F}\log\left(\frac{c_{HAH^+}^o}{c_{HA}^w}\right) \qquad (10)$$

$$\Delta_o^w\phi = \Delta_o^w\phi_{A^-}^{0'} + \frac{2.303RT}{F}(\mathrm{pH} - \mathrm{p}K_{a3}^w) + \frac{2.303RT}{F}\log\left(\frac{c_{HA}^w}{c_{A^-}^o}\right) \qquad (11)$$

Because of the dependence of $c_{H^+}^o$ on both potential and pH, the boundary lines corresponding to the various pK_a^o are not vertical but oblique lines which increase by a factor $2.303RT/F$[V] per pH unit, *i.e.* 59 mV/pH unit at 25 °C.

The nature of the various species appearing in the above relationships shows that not all the boundaries are defined as yet. The ionic partition diagram is then completed by using eqs 2−11 to introduce the missing concentration ratios in the expression of the potential and to deduce the missing equiconcentration lines (see Supporting Information for further details).

The final determination of the ionic partition diagram is then accomplished by calculating the coordinates of all the intersection points connecting the various boundaries.

3. Application to the Ionizable Drug Quinidine

The organic drug quinidine[11] is a particular case of the above model. Quinidine contains two amino groups which are basic and one hydroxyl group, as shown by its chemical structure[11] represented in Figure 2. In aqueous acidic solution, it can form soluble singly protonated (HQH^+) or doubly protonated (HQH_2^{2+}) species, but it can also be deprotonated under very basic conditions to form Q^-. In a two-phase system such as water/1,2-dichloroethane, all of these species can be present *a priori* in both phases. The resulting equilibria may thus be described by the same thermodynamic cycle as in Figure 1.

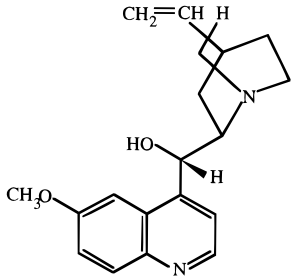

Figure 2. Structure of quinidine (HQ).

3.1. Material and Methods. The aqueous and organic phase solvents were deionized water (Milli-Q) from Millipore, Switzerland, and 1,2-dichloroethane (1,2-DCE) from Merck, Switzerland, respectively. 1,2-DCE was used without further purification and handled with all necessary precautions.[12] Quinidine was obtained from Sigma (U.K.), and potassium chloride, tetrabutylammonium chloride (TBACl), and tetramethylammonium sulfate were supplied by Fluka (CH). Tetrabutylammonium tetrakis(4-chlorophenyl)borate (TBATPBCl) was prepared by methatesis of TBACl with potassium tetrakis(4-chlorophenyl)borate (KTPBCl) obtained from Lancaster (U.K.) and recrystallized twice from methanol. All the reagents used were analytical grade or purer.

The experimental setup was as described in ref 5. All experiments were carried out at room temperature (21 ± 1 °C). Cyclic voltammetry, at various scan rates, was performed on the following electrochemical cell with full iR compensation:

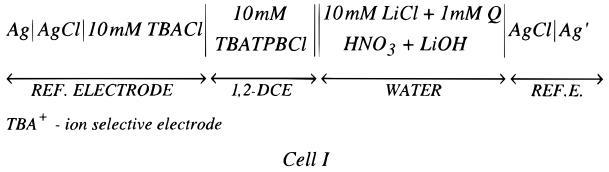

Cell I

For further details on experiments and interpretation of transfer waves, see a previous work.[5]

3.2. Experimental Results. In order to draw the ionic distribution diagram of quinidine, it is necessary to know the values of the formal transfer potentials of the various ions. Cyclic voltammetry was used to this effect and also to determine the nature of the transferring species at any given pH. Figure 3 shows several voltammograms obtained with cell I and representing the transfer of HQH_2^{2+}, HQH^+, and Q^-.

At pH 0.93, only one wave was observed, which was due to the transfer of HQH_2^{2+}. When pH increased, a second peak appeared at a lower potential; the measured current also increased with pH, due to the passage of HQH^+ across the interface. Between pH 6 and 7.5, the peak of HQH_2^{2+} disappeared completely and only the transfer of HQH^+ remained measurable, as shown in Figure 3 by the voltammogram at pH 7.03. Above pH 7.5, a third wave appeared and could be attributed to the transfer of Q^-. It is important to note that the transfer of a cation from the aqueous to the organic phase is defined here as a positive current. This implies that, on the forward scan, the recorded current was due either to the transfer

(11) Doherty, R.; Benson, W. R.; Maienthal, M.; Stewart, J. *J. Pharm. Sci.* **1978**, *67*, 1698−1701.

(12) International program on chemical safety, *1,2-Dichloroethane*, In Environmental Health Criteria, World Health Organization Ed.: Geneva, 1995; Vol. 176, pp 148.

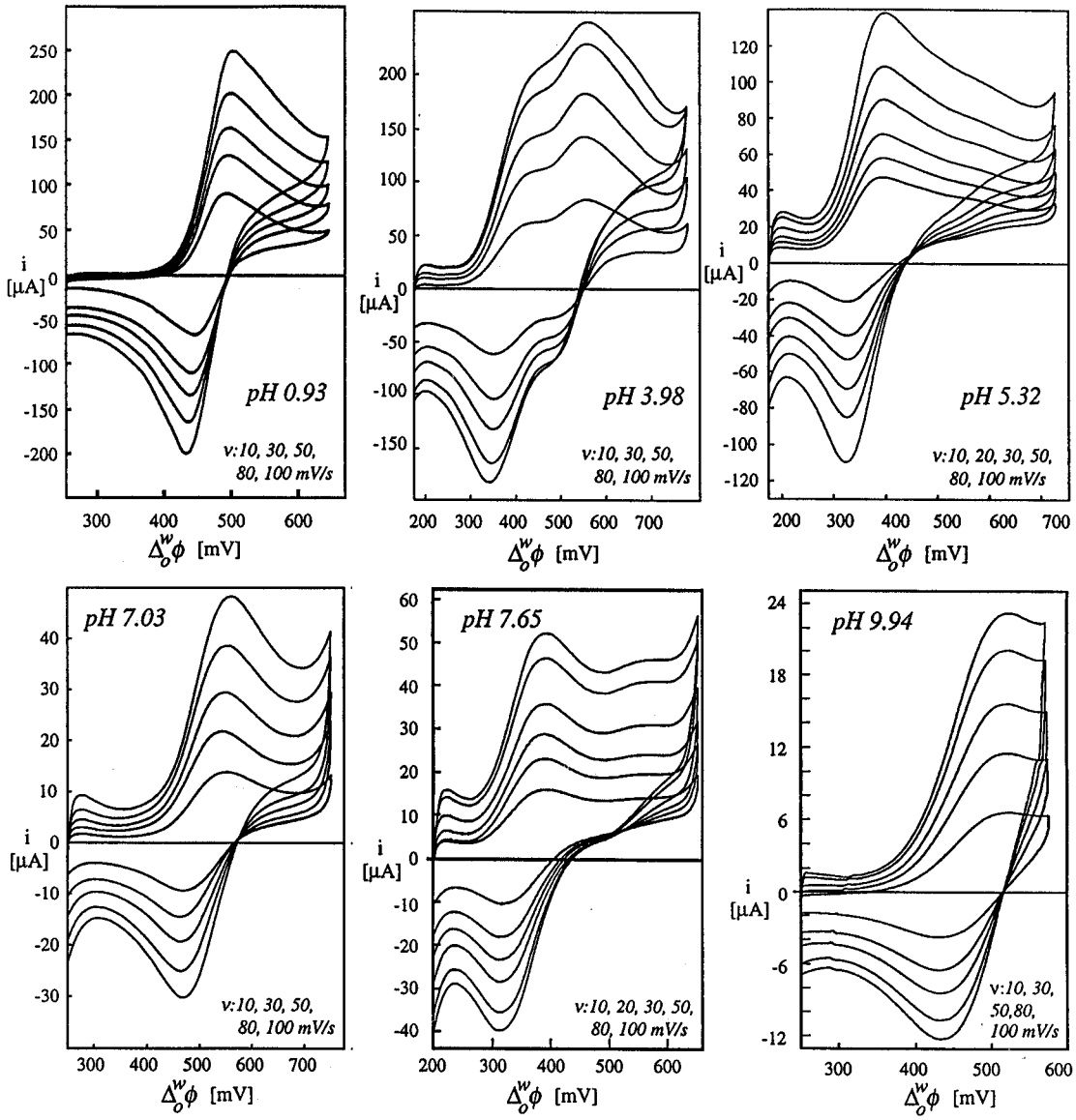

Figure 3. Cyclic voltammograms for the transfer of the various forms of quinidine across the water/1,2-DCE interface at 21 °C. The direction of the forward scan is from left to right (upper part of the curves), and from right to left for the reverse scan.

Table 1. Experimental Results Obtained by Cyclic Voltammetry for the Transfer of Quinidine across the Water/1,2-DCE Interface[a]

	$\Delta_o^w\phi_i^{0'}$	$\Delta G_{tr,i}^{0',w\rightarrow o}$	log P_i^0 [b]	pK_a^w	pK_a^o [c]
HQH_2^{2+}	161.7 ± 3.8	31.2 ± 0.7	−5.54 ± 0.12	4.43 ± 0.02	9.66 ± 0.21
HQH^+	79.8 ± 9.4	7.7 ± 0.9	−1.37 ± 0.16	8.66 ± 0.02	14.20 ± 0.16
Q^-	252.5 ± 18.8	−24.4 ± 1.8	4.33 ± 0.32	17.00 ± 0.50[d]	24.58 ± 0.60[d]

[a] $\Delta_o^w\phi_i^{0'}$ is the formal transfer potential of the ion *i* (given in mV), $\Delta G_{tr,i}^{0',w\rightarrow o}$ its formal Gibbs transfer energy (expressed in kJ/mol), log P_i^0 its standard partition coefficient, and pK_a the dissociation constants in water and in the organic phase, respectively. [b] log P_{HQ} is 2.50 ± 0.04 and was measured by CPC. [c] Calculated by eqs 13−15. [d] Approximated value.

of HQH_2^{2+} or HQH^+ from the water to 1,2-DCE or to that of Q^- from 1,2-DCE to water.

3.3. Drawing the Ionic Partition Diagram of Quinidine. The determination of the ionic partition diagram of quinidine is based partly on results obtained previously[5] and mostly on results reported here. All of the data are summarized in Table 1 to simplify the discussion. Using the procedure described above, it becomes straightforward to calculate the various boundary lines. Table 2 gives all the numerical expressions of these boundaries (deduced from eqs 3, 6, and 9−16 for a temperature of 21 °C), as well as the coordinates of their respective end points. The ionic partition diagram of quinidine can then easily be drawn from Table 2, as represented in Figure 4.

3.4. Discussion. The ionic partition diagrams offer an instantaneous view of how experimental conditions influence the nature of the species in solutions and their transfer, as explained hereafter.

3.4.1. Experimental Domain. The evolution of the potential in Figure 4 is depicted up to a pH value of 26. The domain above pH 14 (line c) is of course beyond experimental reach. Nevertheless, this domain is added to the figure to demonstrate the possible interactions between all the species present. Likewise, very high (as well as very low) potential values cannot be applied across the interface because of secondary reactions which may occur within the cell.

The supporting electrolytes present in cell I may also transfer across the water/1,2-DCE interface. If the applied potential is

Table 2. Equations of the Various Boundary Lines with the Coordinates of Their End Points for Quinidine at 21 °C

no.	concn ratio	boundary lines[a]	first end point[a]	second end point[a]
1	$c^{w}_{HQH_2^{2+}} = c^{o}_{HQH_2^{2+}}$	$\Delta^{w}_{o}\phi = 161.7$	A (0.00; 161.7)	B (3.03; 161.7)
2	$c^{w}_{HQH_2^{2+}} = c^{o}_{HQH^{+}}$	$\Delta^{w}_{o}\phi = 338.4 - 58.4$ pH	B (3.03; 161.7)	C (4.43; 79.8)
3	$c^{w}_{HQH_2^{2+}} = c^{w}_{HQH^{+}}$	pH = 4.43	C (4.43; 79.8)	D (4.43; −728.0)
4	$c^{w}_{HQH_2^{2+}} = c^{o}_{Q^-}$	$\Delta^{w}_{o}\phi = -1503.6 + 175.1$ pH	(0.00; −1503.6)	D (4.43; −728.0)
5	$c^{w}_{HQH^{+}} = c^{o}_{Q^-}$	$\Delta^{w}_{o}\phi = -1245.1 + 116.7$ pH	D (4.43; −728.0)	F (8.66; −234.2)
6	$c^{w}_{HQH^{+}} = c^{o}_{HQH^{+}}$	$\Delta^{w}_{o}\phi = 79.8$	C (4.43; 79.8)	E (8.66; 79.8)
7	$c^{o}_{HQH_2^{2+}} = c^{o}_{HQH^{+}}$	$\Delta^{w}_{o}\phi = -14.9 + 58.4$ pH	B (3.03; 161.7)	I (24.04; 1387.9)
8	$c^{w}_{HQH^{+}} = c^{w}_{HQ}$	pH = 8.66	E (8.66; 79.8)	F (8.66; −234.2)
9	$c^{w}_{HQ} = c^{o}_{HQH^{+}}$	$\Delta^{w}_{o}\phi = -425.6 + 58.4$ pH	E (8.66; 79.8)	G (17.00; 566.5)
10	$c^{w}_{HQ} = c^{o}_{Q^-}$	$\Delta^{w}_{o}\phi = -739.7 + 58.4$ pH	F (8.66; −234.2)	H (17.00; 252.5)
11	$c^{w}_{HQ} = c^{w}_{Q^-}$	pH = 17.00	G (17.00; 566.5)	H (17.00; 252.5)
12	$c^{w}_{Q^-} = c^{o}_{Q^-}$	$\Delta^{w}_{o}\phi = 252.5$	H (17.00; 252.5)	K (26.00; 252.5)
13	$c^{w}_{Q^-} = c^{o}_{HQH^{+}}$	$\Delta^{w}_{o}\phi = -1417.8 + 116.7$ pH	G (17.00; 566.5)	I (24.04; 1387.9)
14	$c^{w}_{Q^-} = c^{o}_{HQH_2^{2+}}$	$\Delta^{w}_{o}\phi = -716.4 + 87.5$ pH	I (24.04; 1387.9)	J (26.00; 1559.8)

[a] With $\Delta^{w}_{o}\phi$ expressed in mV.

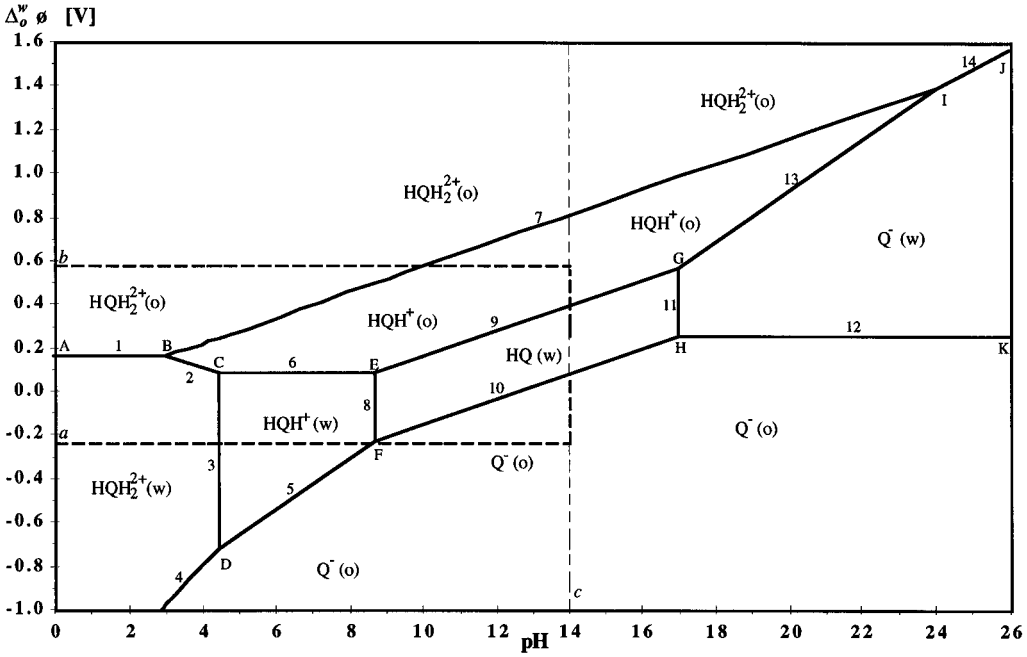

Figure 4. Ionic distribution diagram of quinidine at 21 °C.

highly positive, Li^+ can transfer from water to 1,2-DCE because its transfer potential is reached first ($\Delta^{w}_{o}\phi^{0'}_{Li^+} = 576$ mV[13]). Li^+ limits the potential window and thus the experimental domain of the ionic distribution diagram at positive potentials. Conversely, if $\Delta^{w}_{o}\phi$ is made very negative, then TBA^+ can transfer from 1,2-DCE to water, which limits the potential window at negative potentials ($\Delta^{w}_{o}\phi^{0'}_{TBA^+} = -230$ mV[13]). Hence, the bold broken lines in Figure 4 constitute the working domain which can effectively be reached experimentally, lines a and b defining the potential limits beyond which Li^+ and TBA^+ transfer preferentially.

The potential window can be enlarged toward negative values, if bis(triphenylphosphoranylidene)ammonium tetrakis(4-chlorophenyl)borate (BTPPATPBCl) is used as supporting electrolyte in the organic phase instead of TBATPBCl. Indeed, in this case, the potential window becomes limited by the transfer of the chloride ions ($\Delta^{w}_{o}\phi^{0'}_{Cl^-} = -526$ mV[14]), expanding the experimental domain to very low potentials. This should allow the detection of Q^- at pH 7 already.

3.4.2. Transfer Mechanisms. The ionic partition diagrams allow a direct interpretation of the mechanisms governing the transfer of the various species upon variation of the Galvani potential difference and/or aqueous pH, as can be demonstrated from Figure 4 in the case of quinidine.

For uncharged interfaces, *i.e.* when $\Delta^{w}_{o}\phi = 0$, the predominant species upon increase of pH are respectively HQH_2^{2+}(w), HQH^+(w), HQ(w), and Q^-(o). If the first three are intuitively predictable, the last one is not as intuitively obvious. Indeed, with an aqueous pK_a of about 17 for the alcohol group, one would not expect the anion to be the predominant species in the organic phase. However, this result shows that in the organic phase quinidine is anionic when the adjacent aqueous pH is greater than about 12.

At very low pH (*e.g.*, pH = 1) and low potential, HQH_2^{2+}(w) is predominant. If the Galvani potential difference is increased, the doubly charged quinidine is forced through the interface, since the potential of water with respect to the organic phase is made increasingly positive. The increase of $\Delta^{w}_{o}\phi$ then favors

(13) Shao, Y.; Stewart, A. A.; Girault, H. H. *J. Chem. Soc., Faraday Trans.* **1991**, *87*, 2593−2597.

(14) Sabela, A.; Marecek, V.; Samec, Z.; Fuoco, R. *Electrochim. Acta* **1992**, *37*, 231−235.

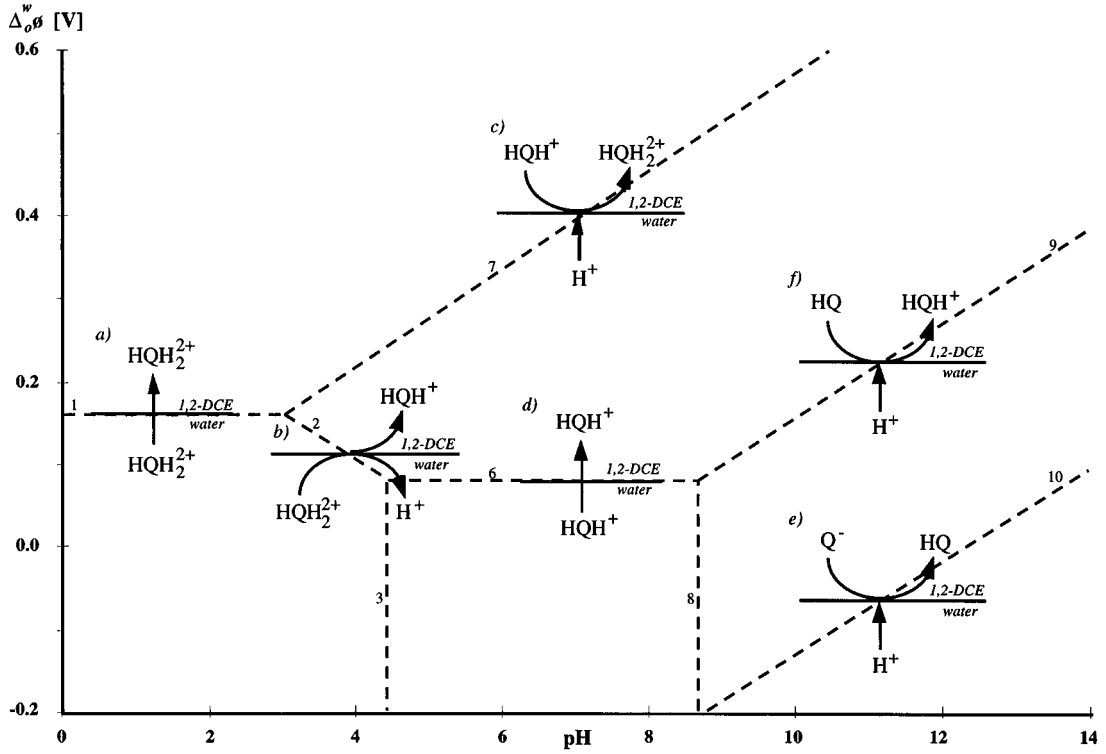

Figure 5. Schematic transfer mechanisms of the various forms of quinidine at the water/1,2-DCE interface. The following transfers are outlined: (a) simple HQH_2^{2+} transfer; (b) HQH_2^{2+} transfer by interfacial dissociation; (c) assisted proton transfer facilitated by HQH^+(o); (d) simple HQH^+ transfer; (e) assisted proton transfer facilitated by Q^-; (f) assisted proton transfer facilitated by HQ(o).

the presence of HQH_2^{2+}(o) whose concentration becomes equal to that of HQH_2^{2+}(w) when the boundary line 1 is reached. This generates a flux of ions across the water/1,2-DCE interface, which can be experimentally observed as an anodic current as schematically illustrated in Figure 5a.

Between pH 3 and 4.5, a very interesting phenomenon occurs. At low potential, HQH_2^{2+}(w) is still the predominant species. However, when $\Delta_0^w\phi$ increases, the doubly charged quinidine loses a proton upon transfer to the organic phase, and HQH^+(o) is the predominant species for slightly positive potentials. Such a mechanism is similar to the transfer by interfacial dissociation (TID mechanism) of assisted ion transfer reactions[15] and is illustrated in Figure 5b. Upon further increase of potential, HQH^+(o) acts as a proton acceptor, facilitating the transfer of a proton into the organic phase, which yields HQH_2^{2+}(o) again (see Figure 5c). These data show that there are two paths to the overall transfer of HQH_2^{2+}(w) from water to the organic phase: one by direct transfer at low pH, and one by deprotonation/transfer, followed by proton transfer facilitated by HQH^+(o).

For pH comprised between 4.5 and 8.5, the predominant species at low potential is HQH^+(w). An increase of potential results in a simple transfer of HQH^+, as shown in Figure 5d. As previously, once HQH^+ is in 1,2-DCE, a further polarization let it accept a proton coming from the aqueous phase. This transfer proceeds by interfacial complexation (TIC mechanism)[15] as depicted in Figure 5c, and the resulting current is due to the passage of the proton across the interface. In other words, HQH^+(o) acts as a "proton pump" in this range of pH upon increase of potential or proton concentration.

Above pH 9, the predominant species is Q^-(o) at negative potentials. Consequently, when the water is negatively polarized with respect to the organic phase, quinidine in the organic phase becomes an organic acid giving its proton to the aqueous phase and the base Q^- staying in the organic phase. Oppositely, upon increase of polarization, this anion can act as a proton acceptor to yield the neutral quinidine in the organic phase (see Figure 5e). In turn, HQ(o) and HQH^+(o) can both act as proton acceptors upon increase of polarization to yield HQH^+(o) (Figure 5f) and HQH_2^{2+}(o) (Figure 5c), respectively.

3.4.3. Lipophilicity. The ionic partition diagram illustrates the lipophilicity of the different species present: the boundaries corresponding directly to the reactions of transfer (lines 1, 6, and 12) allow comparison of the energy required by these ions to cross the water/1,2-DCE interface. It can be deduced from Figure 4 that Q^- and HQ are lipophilic species, since they have a more negative solvation energy in 1,2-DCE than in water, and therefore require energy to pass from 1,2-DCE into water. By contrast, HQH_2^{2+} and HQH^+ are hydrophilic species. Their hydration energy is more negative than their solvation energy, so that they are better stabilized in water than in 1,2-DCE and need energy to pass from the aqueous phase into the organic phase. Moreover, as expected, HQH_2^{2+} is more hydrophilic than HQH^+, as can be seen by line 1 in the ionic partition diagram, which is positioned at a larger value of $\Delta_0^w\phi$ than line 6, and by the values of log P_i^0 given in Table 1.

These considerations are of great interest for structure−permeation relationship studies,[16−19] since the lipophilicity of ions was generally neglected in the models describing the disposition of drugs. However, 1,2-DCE was used instead of

(15) Shao, Y.; Osborne, M. D.; Girault, H. H. *J. Electroanal. Chem.* **1991**, *318*, 101−109.

(16) Kubinyi, H. QSAR: Hansch Analysis and Related Approaches. In *Methods and Principles in Medicinal Chemistry*; Mannhold, R., Krogsgaard-Larsen, P., Timmerman, H., Eds.; VCH: Weinheim, Germany, 1993; Vol. 1, pp 240.

(17) Roberts, M. S.; Pugh, W. J.; Hadgraft, J.; Watkinson, A. C. *Int. J. Pharm.* **1995**, *126*, 219−233.

(18) Pliska, V. The Role of Lipophilicity in Biological Response to Drugs and Endogenous Ligands. In *Lipophilicity in Drug Action and Toxicology*; Pliska, V., Testa, B., van de Waterbeemd, Eds.; VCH: Weinheim, Germany, 1996; Vol. 4, pp 263−293.

(19) Smith, D. A.; Jones, B. C.; Walker, D. K. *Med. Res. Rev.* **1996**, *16*, 243−266.

the solvents traditionally used in lipophilicity measurements (n-octanol and alkanes[20]) because of experimental facilities in polarizing the interface. Nevertheless, recent studies[21] show that the water/1,2-DCE solvent system could be an interesting complement to the water/*n*-octanol system in the search of simple models for biological membranes. Indeed, H-bond interactions, which are described as an important factor for the passive diffusion across membrane,[22] are the main intermolecular forces governing the partitioning in the water/1,2-DCE system.[21] In this manner, lipophilicity measurements with a polar solvent such as 1,2-DCE is also a means of better understanding membrane permeation by drugs.

4. Conclusion

The methodology described in this paper applies to any ionizable solute and to any biphasic liquid/liquid system. Being independent of the concentration of the various species present, ionic distribution diagrams are valid under any experimental conditions. They constitute a rather simple way to visualize all the species present at the ITIES, to predict the nature of the transferring species, and to describe the transfer mechanisms of ionizable solutes.

This last point is of great significance to understand how drugs can cross cellular membranes to reach their biological targets or to leave cells. Ionic partition diagrams allow one to predict which form an ionic solute will take as it transfers under given conditions of potential and pH. In the same manner, they allow one to quantitate the lipophilicity of the various forms of a solute, as well as to predict their most stable electrical states.

Acknowledgment. P.-A.C., H.G., and B.T. are grateful for support by the Swiss National Science Foundation.

Supporting Information Available: Theoretical development of ionic partition diagrams (10 pages). See any current masthead page for ordering and Internet access instructions.

JA962187T

(20) Dearden, J. C.; Bresnen, G. M. *Quant. Struct.-Act. Relat.* **1988**, *7*, 133−144.
(21) Steyaert, G.; Lisa, G.; Gaillard, P.; Boss, G.; Reymond, F.; Girault, H. H.; Carrupt, P.-A.; Testa, B. Submitted for publication.
(22) Roberts, M. S.; Pugh, W. J.; Hadgraft, J. *Int. J. Pharm.* **1996**, *132*, 23−32.